Aromatic and Cation−π Interactions Enhance Helix−Helix Association in a Membrane Environment†

Rachel M. Johnson,‡,§ Karen Hecht,‡,§ and Charles M. Deber*,‡,§

Division of Molecular Structure and Function, Research Institute, Hospital for Sick Children, Toronto, Ontario, Canada M5G 1X8, and Department of Biochemistry, University of Toronto, Toronto, Ontario, Canada M5S 1A8

Received May 9, 2007; Revised Manuscript Received June 8, 2007

ABSTRACT: The cation−π interaction is an electrostatic attraction between a positive charge and the conjugated π electrons of an aromatic ring. These interactions are well documented in soluble proteins and can be both structurally and functionally important. Catalyzed by observations in our laboratory that an Ala- and Ile-rich two-helix transmembrane segment tended to form SDS-resistant dimers upon the incorporation of suitably located Trp residues, here we have constructed a library of related constructs to study systematically the impact of aromatic−aromatic and cation−π interactions on tertiary structure formation within an *Escherichia coli* membrane. Using the TOXCAT oligomerization assay with the hydrophobic segment AIAIAIIAZAXAIIAIAIAI, where Z = A, W, Y, or F and X = A, H, R, or K in all possible combinations of cation and/or aromatic pairings, to assess the TM−TM dependent expression of the chloramphenicol acetyltransferase reporter gene, we find that cation−π interactions, particularly between Lys and Trp, Tyr, or Phe, as well as weakly polar interactions between pairs of aromatic residues, significantly enhance the strength of oligomerization of these hydrophobic helices, in some instances forming oligomers four times stronger than the high-affinity glycophorin A dimer. The contribution of these forces to the tertiary structure formation in designed transmembrane segments suggests that similar forces may also be a significant factor in the folding and stability of native membrane proteins.

Membrane proteins comprise a third of the total protein content of a cell and play important roles in numerous biological functions such as receptor signaling, ion conductance, and nutrient transport (*1*). Compared to their soluble counterparts, relatively little structural information is available on membrane proteins due to challenges inherent in their hydrophobic nature (*2*). However, in membrane protein folding as described by the two-stage model (*3*−*5*), transmembrane (TM)[1] segments are depicted as individually stable, self-folding units that interact with one another to form the final folded structure. In this process, formation of tertiary and quaternary structure must accordingly involve helix−helix association through noncovalent forces, believed to be largely van der Waals packing and electrostatic forces (*6*). Van der Waals packing mediates helix−helix association by maximizing the surface area of contact between helices, typically using small residue packing motifs such as GxxxG and AxxxA (*7*−*10*). Electrostatic interactions stabilize folded structures via polar side chain−side chain or side chain−backbone interactions between interacting helices (*11*−*16*).

However, other important subsets of noncovalent interactions in both soluble and membrane protein structural biology have emerged and involve aromatic interactions, either between two aromatic residues ($\pi-\pi$) or between a basic and an aromatic residue (cation−π). Aromatic rings (i.e., Trp, Phe, and Tyr) and their self-association or interaction with cations (i.e., Arg, Lys, and His) have been proposed to consist of van der Waals and electrostatic forces (*17*, *18*); however, the relative contribution and magnitude of each of these components are still under current investigation. Correct packing geometry contributes to the van der Waals component, whereas the electrostatic component is believed to arise from interactions with the quadrupole moment of the aromatic ring. Two orientations are typically found for $\pi-\pi$ interactions (Figure 1a,b): the edge-face and offset stacked geometries (*18*). The edge-face geometry can be considered a CH−π interaction and is commonly observed between aromatic residues in proteins. The offset stacked geometry acts to bury more surface area, resulting in increased van der Waals and hydrophobic interactions. Similarly for cation−π interactions (Figure 1c,d), there are two preferred geometries (parallel and perpendicular) of the charged (often amino) group in relation to the electron-rich face of the aromatic ring, where the parallel conformation is typically favored by a 2.5:1 ratio (*19*). Since aromatic interactions

† This work was supported, in part, by a grant to C.M.D. from the Canadian Institutes of Health Research (CIHR). R.M.J. was the recipient of an Ontario Graduate Scholarship and a Research Training Committee award from the Hospital for Sick Children. K.H. was a participant in the Samuel B. Lunenfeld Summer Student Program at the Research Institute, Hospital for Sick Children.

* Address correspondence to this author at the Hospital for Sick Children. Phone: 416-813-5924. Fax: 416-813-5005. E-mail: deber@sickkids.ca.

‡ Hospital for Sick Children.

§ University of Toronto.

[1] Abbreviations: TM, transmembrane; GLRA1, human glycine receptor; SDS−PAGE, sodium dodecyl sulfate−polyacrylamide gel electrophoresis; MBP, maltose binding protein; CAT, chloramphenicol acetyltransferase; GpA, glycophorin A; gp55-P, the envelope protein of the polycythemic strain of the spleen focus forming virus; BNIP3, the mitochondrial proapoptotic protein Bcl-2/19 kDa interacting protein; HRP, horseradish peroxidase; ELISA, enzyme-linked immunosorbent assay.

10.1021/bi7008773 CCC: $37.00
Published on Web 07/21/2007

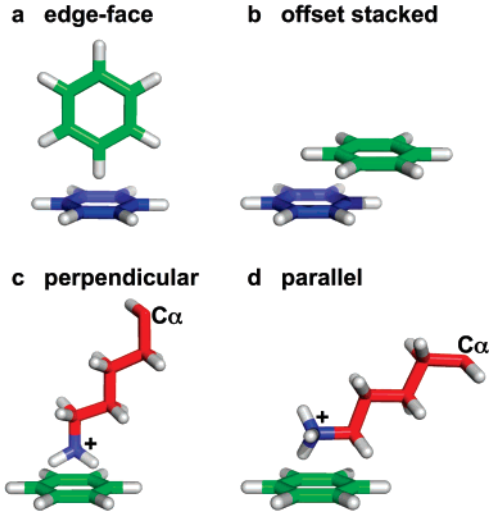

FIGURE 1: Geometries of aromatic and cation−π interactions. Aromatic interactions adopt either (a) edge-face or (b) offset stacked geometries. Carbon atoms are colored in green (atoms in first Phe side chain) or blue (atoms in second Phe side chain) in panels a and b. Cation−π interactions adopt either (c) perpendicular or (d) parallel geometries. Carbon atoms are colored in red (Lys side chain atoms) or green (Phe side chain atoms). This figure was created using PyMol (http://www.pymol.org). Hydrogen atoms are colored in white in all panels; nitrogen atoms are rendered in blue in panels c and d.

consist of both van der Waals forces and electrostatic interactions, Trp, Tyr, and Phe residues provide a potential interaction site that is polar yet also hydrophobic, a combination of properties that is especially suitable for the interior of a globular protein or for the plasma membrane.

The importance of aromatic and cation−π interactions in membrane proteins has been examined by theoretical and experimental methods. For example, a randomization study found that Trp specifically mediated strong in vivo association of transmembrane segments based on a heptad repeat pattern ([***a***XX***de***X***g***]$_n$) of amino acids, which is known from soluble leucine zipper interaction domains (*20*). Furthermore, the cation−π forming residue Tyr381 in the TM domain of the acetylcholine receptor plays a key role in receptor function (*21*). Cation−π interactions between Arg and Trp have also been shown to stabilize a protein/polypeptide in the lipid bilayer (*22*). Studies aimed at examining cation−π interactions from the crystal structures of α-helical membrane proteins have shown that such interactions play a significant role in stabilizing membrane protein structures, where the electrostatic component of the interaction energy is twice that of the van der Waals energy (*23*−*26*) and the overall average energetic contribution from cation−π pairs was approximately −6.5 kcal/mol (*23*). In the same study, it was also observed that cation−π interactions occurred with no specific preference for location and were found between residues in the transmembrane helices, outside of the membrane, or between membrane-bound and surface residues in the loop regions (*23*).

The residues involved in cation−π interactions are also highly conserved (*24*). Interestingly, there are several human diseases involving membrane proteins for which the phenotypic point mutations appear to occur in the context of a disrupted cation−π pair or the introduction of a non-native cation−π interaction. Notably, the most frequent mutations in the human glycine receptor (GLRA1), leading to startle disease, occur at positively charged or aromatic residues in the TM2 domain (K276E, Y279C, R271L, R271Q, and Q266H) (*27*). Although no specific structural data are available for GLRA1, the likelihood of interhelical cation−π bonding is significant, considering the frequency with which aromatic residues occur in the surrounding TM domains (Figure 2).

We previously demonstrated the existence of cation−π interactions in helix−helix association in vitro using a hydrophobic helical hairpin, a minimal tertiary folding helix−turn−helix model termed AI (*2*). This AI hairpin used "small" (Ala) and "large" (Ile) residues to maximize tertiary contacts between the two antiparallel helical TM segments (*2*). In this context, oligomerization assays by SDS−PAGE analysis showed that a strategically located Arg, His, or Lys residue on one hairpin was interacting with the Trp residue on another hairpin, resulting in a four-helix bundle SDS-resistant dimer; dimerization was abrogated in Trp-knockout mutants. To enhance our understanding of these phenomena, we examine here systematically the contribution of aromatic and cation−π interactions to membrane-based helix−helix association in vivo, by using the TOXCAT assay (*28*) in the context of a single AI-like transmembrane helix peptide of prototypic sequence AIAIAIIAZAXAIIAIAIAI (*2*), where Z = A, W, Y, or F and X = A, K, R, or H, representing all possible aromatic and/or cationic residue combinations.

EXPERIMENTAL PROCEDURES

Vectors and Strains. The expression vectors pccKan, pccGpA-WT, and pccGpA-G83I, along with *Escherichia coli* strain NT326, were kindly provided by Dr. Donald Engelman, Yale University (*28*). The TOXCAT constructs contain an N-terminal ToxR DNA binding domain, a transmembrane domain, and a periplasmic maltose binding protein (MBP) domain. Construction of pccAI-WT (WAI) has been described elsewhere (*2*). Individual mutants were produced by mutating the WAI construct using the QuikChange site-directed mutagenesis kit (Stratagene, La Jolla, CA). The sequences of all constructs were confirmed using DNA sequencing. Constructs were subsequently transformed into *E. coli* NT 326 (*malE*-) cells. Whole cell lysates were used to determine expression levels of the constructs. Western blotting was used to analyze samples using an antibody against MBP (New England Biolabs, Beverly, MA). The blot was developed using a goat anti-rabbit horseradish peroxidase (HRP) secondary antibody (Sigma, St. Louis, MO), and band densitometry was performed using NIH image. Statistical analysis was performed using the software program R (*29*).

Chloramphenicol Acetyltransferase (CAT) Enzyme-Linked Immunosorbent Assay (ELISA). Constructs transformed into NT 326 cells were grown at 37 °C in a shaker at 250 rpm to an A_{600} of 0.6. Cells were harvested in 1 mL fractions and stored at −80 °C. Cell lysates were prepared as previously described (*30*). The cell lysate was assayed for CAT concentrations using the CAT ELISA kit (Roche Applied Science, Indianapolis, IN). A standard curve was generated with CAT provided by the supplier. In each experiment, the high-affinity GpA homodimer and a mutant that disrupts dimerization of GpA (G83I) were included as controls. All measurements were performed in at least triplicate, and errors shown are standard deviations on at least three measurements.

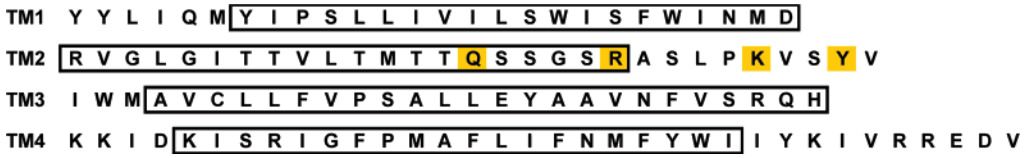

FIGURE 2: GLRA1 transmembrane domain sequences. Residues that are buried within the hydrophobic bilayer are boxed, and residues subject to phenotypic mutations are highlighted in gold.

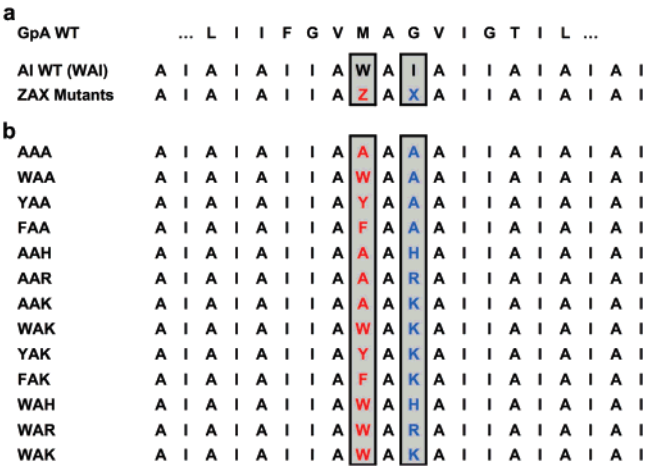

FIGURE 3: Construct design and sequence alignment of AI aromatic and/or basic residue constructs. (a) WT GpA and WT AI (WAI) sequences are shown, along with the design of ZAX mutants. (b) Sequences of ZAX mutants are shown. Gray boxes represent the mutation positions, where aromatic residue positions are highlighted in red (Z = A, W, Y, or F) and the basic residue positions are highlighted in blue (X = A, H, K, or R).

Statistical analysis was performed using the R software program (*29*).

MalE Complementation Test. M9 minimal medium plates were used with 0.4% maltose as the only carbon source (*28*). NT 326 cells transformed with each mutant were streaked onto the plates and incubated for 2 days at 37 °C.

RESULTS

Transmembrane helix sequences including WT AI (WAI), and AI mutants (ZAX) representing aromatic (Trp, Tyr, and Phe) and/or cationic residue combinations (His, Arg, and Lys) (Figure 3) were incorporated into the TOXCAT vector pccKAN and expressed in the inner membrane of *E. coli* with an N-terminal fusion of the DNA binding domain of ToxR, and a C-terminal fusion of the periplasmic maltose binding protein (MBP) domain (*28*). The separation of the X and Z sites in the construct by a single (Ala) residue mitigates against their preferential interaction within a single helix, while simultaneously orienting both X and Z side chains toward an incipient helix−helix interface. The well-studied glycophorin A (GpA) TM segment was included in our studies as a reference high-affinity dimer (*9*, *31*). In the TOXCAT system, ToxR domain dimerization is driven by the homooligomerization of the TM domain, resulting in transcriptional activation of a CAT reporter gene. The extent of TM helix-mediated association can therefore be measured, as it correlates to the level of CAT expression. TOXCAT does not provide a measure of the order of the oligomers formed; however, it is a powerful tool for assessing the relative strength of TM helix interactions in a natural membrane bilayer (*32*). A GpA mutant, G83I, known to disrupt helix−helix association, was used as a negative control for oligomerization (not shown).

The correct membrane insertion of each fusion protein was confirmed by growth of NT 326 cells expressing each fusion protein construct on M9-maltose plates (not shown). Western blotting and densitometry measurements (*2*, *8*, *28*, *30*, *33*−*41*) were used to confirm that the expression levels of each chimera were produced at comparable levels (Figure 4). Since the expression levels of all fusion proteins were similar, any differences in the CAT expression levels can be considered to be the result of relative dimer affinity.

Two constructs, WAI and AAA, were initially tested for their CAT expression levels in comparison to the high-affinity GpA dimer. As previously observed, WAI exhibited a similar CAT concentration to WT GpA ($p = 0.102$ for GpA vs WAI) (Figure 4), indicating that WAI similarly associates through its TM helix with high affinity. On the other hand, AAA had approximately 64% of the CAT signal compared to WT GpA (Figure 4), indicating that AAA dimerizes but at a lower affinity than both WT GpA and WAI ($p = 0.003$ for GpA vs AAA). The decrease in CAT signal likely results from the loss of an aromatic residue (vide infra); however, the removal of an Ile residue from the TM−TM van der Waals packing interface could also result in some decrease in CAT signal.

Aromatic-Substituted Constructs Oligomerize with Higher Affinity Than WT GpA, and Their Affinities Are Dependent on both Steric and Electrostatic Constraints. The observed difference in dimerization levels of WAI and AAA led us to investigate the role of aromatic residues in the TM−TM oligomerization of the AI construct. Three chimeras (WAA, FAA, and YAA) were constructed, and their ability to facilitate helix−helix association was tested in the TOXCAT assay (Figure 4a). All three constructs displayed CAT signals higher than WAI, where FAA had the highest signal followed by YAA and then WAA. WAA and WAI differ by only one residue (Ile), yet their CAT signals are significantly different, indicating that the loss of a "knob" in the van der Waals interface (WAA) is likely contributing to its lower affinity as compared to WAI.

Interestingly, the TOXCAT signal appears to increase as the volume of the aromatic side chain decreases (i.e., FAA > YAA > WAA). Furthermore, the electrostatic potential surface for each of the three aromatic residues differs, where Trp has the largest surface of negative charge above and below the plane of the aromatic ring, followed by Tyr and Phe (*17*). Both the residue volume and its electrostatic potential surface suggest that the dimerization of these constructs depends on both steric constraints as well as charge−charge repulsion.

Basic Residues Facilitate Strong Helix−Helix Associations in AI. The role of basic residues in the helix−helix association of AI was determined by examining the CAT levels of three chimeras, AAR, AAK, and AAH (Figure 4b).

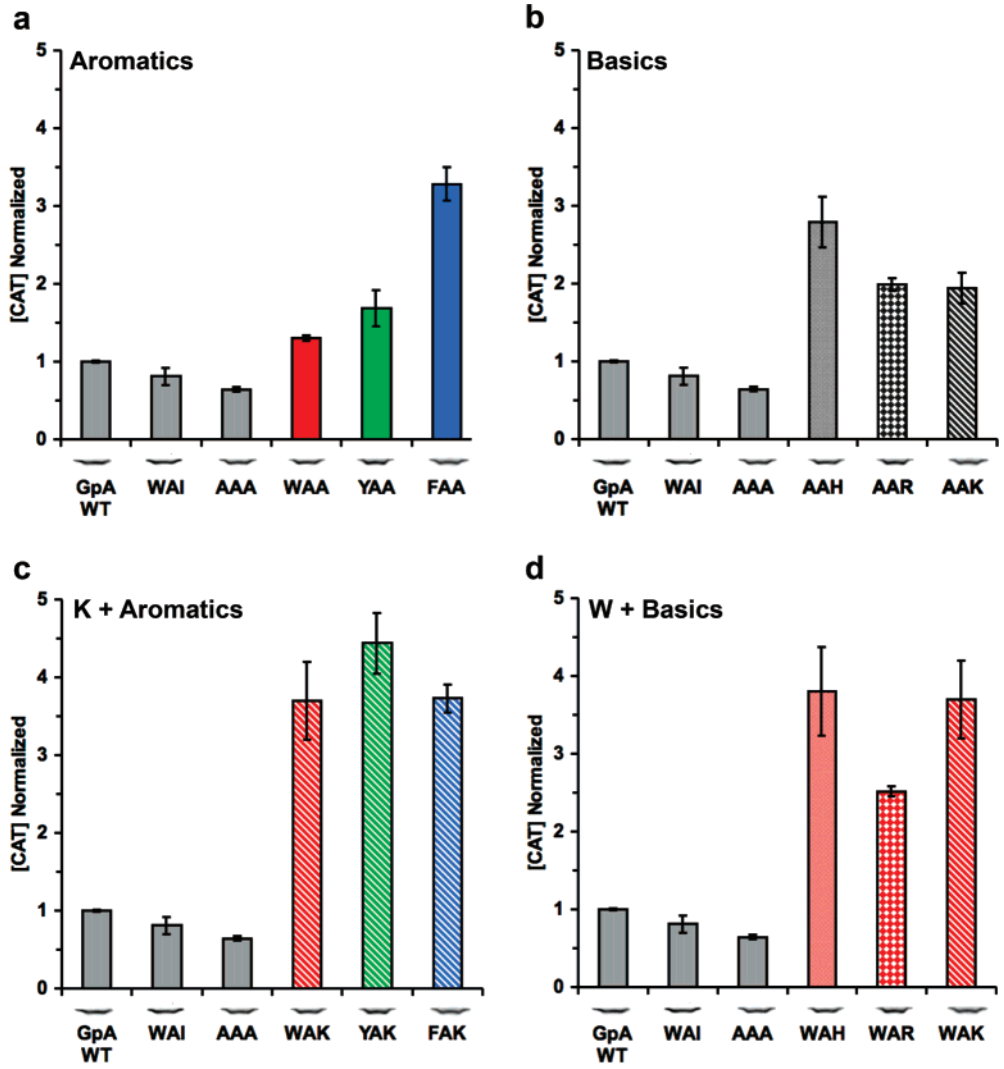

FIGURE 4: TOXCAT assay of WT GpA and the AI aromatic and basic residue-substituted series. CAT expression is normalized to WT GpA and is shown for the following series: (a) aromatics; (b) basics; (c) Lys and aromatics; (d) Trp and basics. Aromatic residue substitutions are colored in red (Trp), green (Tyr), or blue (Phe). Basic residue substitutions are shaded with a solid (His), diamond (Arg), or stripe (Lys) pattern. Aromatic and basic residue substituted constructs [prototypic sequence: AIAIAIIAZAXAIIAIAIAI (*2*), where Z = A, W, Y, or F and X = A, K, H, or R] are colored and shaded with the appropriate combinations; for example, WAK is colored red (Trp) and is shaded with a striped pattern (Lys). Error bars represent the standard deviation of at least three separate measurements. Fusion protein expression levels are shown below each graph, where cell lysates were assayed by Western blot using an anti-MBP antibody.

All constructs exhibited either a 3-fold (AAR and AAK) or 4-fold (AAH) increase in CAT expression levels in comparison to AAA. Thus, even in the absence of aromatic residues, it appears that all three basic residues are able to facilitate TM−TM association in the AI construct. It is interesting to note that AAR and AAK have similar oligomerization levels whereas AAH has a higher reported CAT expression level (Figure 4b). Arg and Lys residues may be able to H-bond interhelically (either side chain−side chain or side chain−backbone) if the pK_a within the membrane is shifted enough to allow the side chains of Arg and Lys to become deprotonated. Depending on its protonation state, His residues are either basic (protonated) or aromatic (deprotonated) in nature (*17*). This means that His can, in principle, participate in both $\pi-\pi$ and cation−π interaction types, as well as H-bonding (when it is deprotonated), likely leading to the observed higher stability than either Arg or Lys.

Cation−π Interactions Contribute to the Stability of the TM−TM Association of AI. Previous in vitro studies (*2*) indicated that Lys and Trp residues were able to participate in cation−π interactions, stabilizing the dimerization of a hydrophobic helical AI hairpin, resulting in a four-helix bundle. To investigate whether similar results can be observed in vivo, we sought to determine the effect of a Lys residue on the association of aromatic residue constructs (WAA, YAA, and FAA). Three chimeras were constructed (WAK, YAK, and FAK), and their CAT levels were determined (Figure 4c). All three constructs reported similar levels within error and were all 4-fold greater than WT GpA, indicating remarkably high dimer affinities. Furthermore, there was a 2.5−3-fold increase in TOXCAT signal for WAK vs WAA ($p = 0.015$) and YAK vs YAA ($p = 0.002$), indicating that the copresence of a Lys residue greatly increases the TM−TM association of W- and Y-containing helices. Interestingly, there was no difference in CAT expression for FAK vs FAA ($p = 0.060$), suggesting that the Lys residue in this case is not likely participating in its helix−helix association per se. An energy-minimized model was produced for the WAK construct, in which cation−π

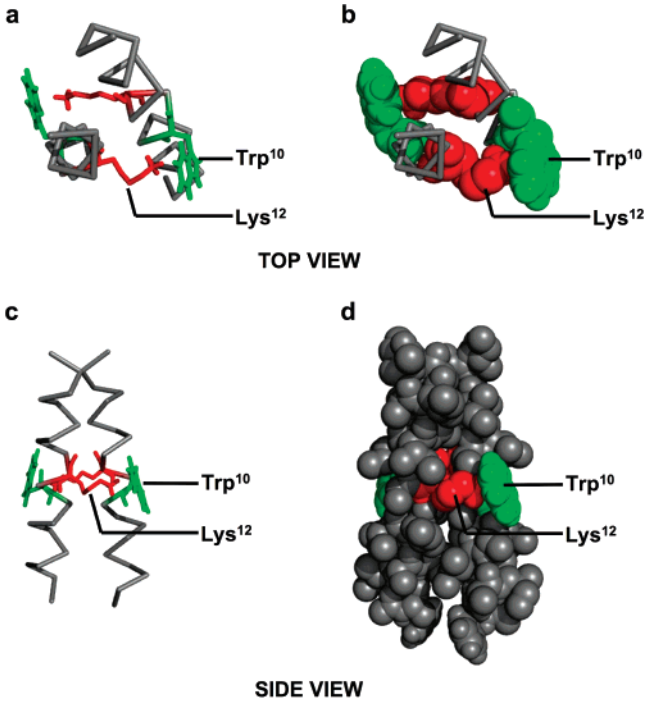

FIGURE 5: Energy-minimized molecular model of a parallel dimer of the WAK construct. This dimeric model was generated using a global conformation search program as previously described (*52*, *53*). Backbone models are shown in (a) and (c); space-filling models are shown in (b) and (d). The Trp^{10} residue is highlighted in green, and the Lys^{12} residue is highlighted in red. Both top views (panels a and b) and side views (panels c and d) are shown. This figure was created using PyMol (http://www.pymol.org).

interactions are observed between the Trp residue on one helix with the Lys residue on the other helix (Figure 5).

In addition, chimeras with Arg and His were constructed with Trp (WAR and WAH) to investigate the effects of various basic residues in the context of an aromatic residue. The CAT signals determined (Figure 4d) showed that WAH, WAK, and WAR all associated at higher strengths than corresponding AAH, AAK, and AAR systems. Interestingly, there was a larger difference between AAK vs WAK and AAH vs WAH (1.5−2-fold) than in AAR vs WAR (p values were 0.030, 0.043, and 0.003, respectively), suggesting that while cation−π interactions specifically contribute to the stability of the TM−TM association of AI, variations arise based on the identity of the interacting pairs.

DISCUSSION

Glycophorin A is known for its strong dimerization potential mediated by a GxxxG sequence motif that permits close contacts between interacting TM helices (*42*). However, TM−TM interactions stronger than those of GpA have been observed using TOXCAT in a number of proteins including gp55-P, the envelope protein of the polycythemic strain of the spleen focus forming virus (*33*), and BNIP3, the mitochondrial proapoptotic protein Bcl-2/19 kDa interacting protein (*43*). The observation of signals higher than WT GpA likely originate from the fact that TOXCAT does not provide a measure of the order of the oligomers formed. This assay, however, is useful as a powerful tool for assessing the relative strength of TM helix interactions in a natural membrane bilayer (*32*). Furthermore, the hierarchy of stabilities for sets of mutants is retained, as previously demonstrated by correlation of TOXCAT data to the free energy of dimerization relative to WT GpA in detergent micelles (*37*). It is therefore perhaps not unexpected that, in the present work, some AI chimeras were observed to have significantly higher CAT expression signals than GpA. Indeed, the level of CAT expression in all AI constructs is at least equal to, or greater than, that resulting from GpA dimerization. In GpA, the packing motif GxxxG helps to maximize the surface area of contact between interacting GpA helices and facilitate van der Waals interactions (*42*). However, the strength of helix−helix association has been shown to be dependent on the sequence of residues neighboring such packing motifs (*44*). For example, large residues may push helices apart, increasing the crossing angle and reducing the contact surface area. Given this sequence dependence, and the presence of several AxxxA packing motifs in each AI helix, it may be suggested that the stronger CAT expression in the designed AI segment is the result of better packing interactions, perhaps stronger than those typically observed in native TM segments.

In AI, the TM−TM interaction is dominated by van der Waals packing, in which geometric complementarity between Ala and Ile residues at the interaction interface allows TM helices to approach one another and maximize the surface area of contact (*2*). This proximity between interacting helices strengthens weak electrostatic attractions mediated by the alignment of temporary electric dipoles in atoms at the helix−helix interface (*45*). However, the argument that AI dimerization is stronger than GpA due exclusively to increased van der Waals packing is diminished by the observation that CAT expression from AAA is significantly weaker than that of GpA WT (Figure 4). Thus, the large gain in CAT expression resulting from AI dimerization must be explicable in terms of additional means of interaction augmenting the packing forces already at work in AI.

Introduction of an aromatic residue into the AI TM sequence adds to the strength of TM−TM association in the cases of WAA, YAA, and FAA. Stacking interactions involving the conjugated π electron systems of aromatic residues likely play a role in this TM−TM interaction. Such weakly polar aromatic interactions are well-known to contribute to the structure and function of soluble proteins such a globins, immunoglobulins, and calcium binding proteins (*46*, *47*) and may well be enhanced in the nonpolar membrane environment. The observation that aromatic interactions do not have an effect as pronounced for WAA as for YAA and FAA might be explained by the asymmetry in electron distribution of the heterocyclic indole side chain compared to the more regular distribution of the phenol side chain in Tyr and the benzene side chain in Phe (*17*). As well, the obstacles to accommodating the relatively large indole side chains in TM−TM helical interfaces may mitigate against helix−helix proximity.

Nevertheless, the strength of AI helix−helix association in the presence of Trp increases dramatically upon inclusion of a cationic residue. Since the contribution of each cation−π interaction depends on the polarizability of interacting residues, their proximity, and orientation (Figure 5), our work confirms that variable levels of increase in TM−TM affinity will indeed arise depending on the identity of the cation−π pair (*48*, *49*). For example, the terminal nitrogen on the side chain of Lys is more strongly polarized than the guanidinium group of Arg and produces a stronger cation−π interaction

with aromatic residues (*50*). Furthermore, the residues surrounding the cation−π pair would likely result in further variability of TM−TM affinity; however, the context dependence of this interaction has yet to be determined.

The significantly stronger CAT signal produced from AI constructs bearing only a cationic residue in comparison to GpA WT may be the result of repulsive electrostatic forces acting to restrict the rotational flexibility of AI helices. This conformational restriction may act to define a more rigid interaction interface based on van der Waals packing. Another more likely possibility is that basic residues, in the absence of an aromatic counterpart, are deprotonated (i.e., the pK_a has been shifted due to the local microenvironment) and can now participate in stabilizing H-bonds, either between two side chains (N−H···N) or between the side chain and the peptide backbone (N−H···O═C). In particular, AAH may produce weakly polar aromatic interactions or H-bonding interactions with the peptide backbone depending on the protonation state of histidine in the membrane (*17*). Use of the GALLEX heterooligomerization assay (*51*) in future work will allow us to distinguish between the two mechanisms of stabilization by cationic residues, by determining whether a single His residue can facilitate oligomerization or whether two such residues are required for TM−TM association.

CONCLUSION

Systematic assessment of hydrophobic helical oligomer formation in *E. coli* membranes has shown that cation−π and aromatic interactions are demonstrably significant in the hydrophobic membrane environment. Thus, a designed transmembrane helix of largely alternating Ala and Ile residues forms equal or stronger oligomers than the known high-affinity dimer GpA. While the principal force mediating this interaction is van der Waals packing, our results confirm that additional electrostatic interactions contribute significantly, particularly when cation−π associations between cationic and aromatic residues, which are known to be a prominent feature of soluble proteins, are detected in the TOXCAT assay. In addition, weakly polar interactions between pairs of aromatic residues also partake in stabilization of the AI helical oligomer. The contribution of these forces to the tertiary structure formation in this hydrophobic TM segment suggests that they may also be a factor in the folding and stability of native membrane proteins.

REFERENCES

1. Boyd, D., Schierle, C., and Beckwith, J. (1998) How many membrane proteins are there?, *Protein Sci. 7*, 201−205.
2. Johnson, R. M., Heslop, C. L., and Deber, C. M. (2004) Hydrophobic helical hairpins: design and packing interactions in membrane environments, *Biochemistry 43*, 14361−14369.
3. Engelman, D. M., Chen, Y., Chin, C. N., Curran, A. R., Dixon, A. M., Dupuy, A. D., Lee, A. S., Lehnert, U., Matthews, E. E., Reshetnyak, Y. K., Senes, A., and Popot, J. L. (2003) Membrane protein folding: beyond the two stage model, *FEBS Lett. 555*, 122−125.
4. Popot, J. L., and Engelman, D. M. (2000) Helical membrane protein folding, stability, and evolution, *Annu. Rev. Biochem. 69*, 881−922.
5. Popot, J. L., and Engelman, D. M. (1990) Membrane protein folding and oligomerization: the two-stage model, *Biochemistry 29*, 4031−4037.
6. Rath, A., and Deber, C. M. (2007) Membrane protein assembly patterns reflect selection for non-proliferative structures, *FEBS Lett. 581*, 1335−1341.
7. Senes, A., Gerstein, M., and Engelman, D. M. (2000) Statistical analysis of amino acid patterns in transmembrane helices: the GxxxG motif occurs frequently and in association with beta-branched residues at neighboring positions, *J. Mol. Biol. 296*, 921−936.
8. Russ, W. P., and Engelman, D. M. (2000) The GxxxG motif: a framework for transmembrane helix-helix association, *J. Mol. Biol. 296*, 911−919.
9. MacKenzie, K. R., Prestegard, J. H., and Engelman, D. M. (1997) A transmembrane helix dimer: structure and implications, *Science 276*, 131−133.
10. DeGrado, W. F., Gratkowski, H., and Lear, J. D. (2003) How do helix-helix interactions help determine the folds of membrane proteins? Perspectives from the study of homo-oligomeric helical bundles, *Protein Sci. 12*, 647−665.
11. Choma, C., Gratkowski, H., Lear, J. D., and DeGrado, W. F. (2000) Asparagine-mediated self-association of a model transmembrane helix, *Nat. Struct. Biol. 7*, 161−166.
12. Gratkowski, H., Lear, J. D., and DeGrado, W. F. (2001) Polar side chains drive the association of model transmembrane peptides, *Proc. Natl. Acad. Sci. U.S.A. 98*, 880−885.
13. Zhou, F. X., Cocco, M. J., Russ, W. P., Brunger, A. T., and Engelman, D. M. (2000) Interhelical hydrogen bonding drives strong interactions in membrane proteins, *Nat. Struct. Biol. 7*, 154−160.
14. Zhou, F. X., Merianos, H. J., Brunger, A. T., and Engelman, D. M. (2001) Polar residues drive association of polyleucine transmembrane helices, *Proc. Natl. Acad. Sci. U.S.A. 98*, 2250−2255.
15. Adamian, L., and Liang, J. (2002) Interhelical hydrogen bonds and spatial motifs in membrane proteins: polar clamps and serine zippers, *Proteins 47*, 209−218.
16. Adamian, L., and Liang, J. (2003) Interhelical hydrogen bonds in transmembrane region are important for function and stability of Ca^{2+}-transporting ATPase, *Cell Biochem. Biophys. 39*, 1−12.
17. Dougherty, D. A. (1996) Cation-pi interactions in chemistry and biology: a new view of benzene, Phe, Tyr, and Trp, *Science 271*, 163−168.
18. Waters, M. L. (2002) Aromatic interactions in model systems, *Curr. Opin. Chem. Biol. 6*, 736−741.
19. Ma, J. C., and Dougherty, D. A. (1997) The cation−π interaction, *Chem. Rev. 97*, 1303−1324.
20. Ridder, A., Skupjen, P., Unterreitmeier, S., and Langosch, D. (2005) Tryptophan supports interaction of transmembrane helices, *J. Mol. Biol. 354*, 894−902.
21. Ward, S. D., Curtis, C. A., and Hulme, E. C. (1999) Alanine-scanning mutagenesis of transmembrane domain 6 of the M(1) muscarinic acetylcholine receptor suggests that Tyr381 plays key roles in receptor function, *Mol. Pharmacol. 56*, 1031−1041.
22. Aliste, M. P., MacCallum, J. L., and Tieleman, D. P. (2003) Molecular dynamics simulations of pentapeptides at interfaces: salt bridge and cation-pi interactions, *Biochemistry 42*, 8976−8987.
23. Gromiha, M. M. (2003) Influence of cation-pi interactions in different folding types of membrane proteins, *Biophys. Chem. 103*, 251−258.
24. Gromiha, M. M., and Suwa, M. (2005) Structural analysis of residues involving cation-pi interactions in different folding types of membrane proteins, *Int. J. Biol. Macromol. 35*, 55−62.
25. Gromiha, M. M., Thomas, S., and Santhosh, C. (2002) Role of cation-pi interactions to the stability of thermophilic proteins, *Prep. Biochem. Biotechnol. 32*, 355−362.
26. Kannan, N., and Vishveshwara, S. (2000) Aromatic clusters: a determinant of thermal stability of thermophilic proteins, *Protein Eng. 13*, 753−761.
27. Bakker, M. J., van Dijk, J. G., van den Maagdenberg, A. M., and Tijssen, M. A. (2006) Startle syndromes, *Lancet Neurol. 5*, 513−524.
28. Russ, W. P., and Engelman, D. M. (1999) TOXCAT: a measure of transmembrane helix association in a biological membrane, *Proc. Natl. Acad. Sci. U.S.A. 96*, 863−868.
29. R Development Core Team (2006) R: A language and environment for statistical computing, R Foundation for Statistical Computing, Vienna, Austria, ISBN 3-900051-07-0, URL http://www.R-project.org.
30. Li, R., Gorelik, R., Nanda, V., Law, P. B., Lear, J. D., DeGrado, W. F., and Bennett, J. S. (2004) Dimerization of the transmem-

brane domain of Integrin alphaIIb subunit in cell membranes, *J. Biol. Chem. 279*, 26666−26673.
31. Lemmon, M. A., Flanagan, J. M., Hunt, J. F., Adair, B. D., Bormann, B. J., Dempsey, C. E., and Engelman, D. M. (1992) Glycophorin A dimerization is driven by specific interactions between transmembrane alpha-helices, *J. Biol. Chem. 267*, 7683−7689.
32. Dixon, A. M., Stanley, B. J., Matthews, E. E., Dawson, J. P., and Engelman, D. M. (2006) Invariant chain transmembrane domain trimerization: a step in MHC class II assembly, *Biochemistry 45*, 5228−5234.
33. Constantinescu, S. N., Keren, T., Russ, W. P., Ubarretxena-Belandia, I., Malka, Y., Kubatzky, K. F., Engelman, D. M., Lodish, H. F., and Henis, Y. I. (2003) The erythropoietin receptor transmembrane domain mediates complex formation with viral anemic and polycythemic gp55 proteins, *J. Biol. Chem. 278*, 43755−43763.
34. Dawson, J. P., Melnyk, R. A., Deber, C. M., and Engelman, D. M. (2003) Sequence context strongly modulates association of polar residues in transmembrane helices, *J. Mol. Biol. 331*, 255−262.
35. Dawson, J. P., Weinger, J. S., and Engelman, D. M. (2002) Motifs of serine and threonine can drive association of transmembrane helices, *J. Mol. Biol. 316*, 799−805.
36. Johnson, R. M., Rath, A., Melnyk, R. A., and Deber, C. M. (2006) Lipid solvation effects contribute to the affinity of Gly-xxx-Gly motif-mediated helix-helix interactions, *Biochemistry 45*, 8507−8515.
37. Johnson, R. M., Rath, A., and Deber, C. M. (2006) The position of the Gly-xxx-Gly motif in transmembrane segments modulates dimer affinity, *Biochem. Cell Biol. 84*, 1006−1012.
38. McClain, M. S., Cao, P., and Cover, T. L. (2001) Amino-terminal hydrophobic region of *Helicobacter pylori* vacuolating cytotoxin (VacA) mediates transmembrane protein dimerization, *Infect. Immun. 69*, 1181−1184.
39. McClain, M. S., Iwamoto, H., Cao, P., Vinion-Dubiel, A. D., Li, Y., Szabo, G., Shao, Z., and Cover, T. L. (2003) Essential role of a GXXXG motif for membrane channel formation by *Helicobacter pylori* vacuolating toxin, *J. Biol. Chem. 278*, 12101−12108.
40. Melnyk, R. A., Kim, S., Curran, A. R., Engelman, D. M., Bowie, J. U., and Deber, C. M. (2004) The affinity of GXXXG motifs in transmembrane helix-helix interactions is modulated by long-range communication, *J. Biol. Chem. 279*, 16591−16597.
41. Mendrola, J. M., Berger, M. B., King, M. C., and Lemmon, M. A. (2002) The single transmembrane domains of ErbB receptors self-associate in cell membranes, *J. Biol. Chem. 277*, 4704−4712.
42. Lemmon, M. A., Treutlein, H. R., Adams, P. D., Brunger, A. T., and Engelman, D. M. (1994) A dimerization motif for transmembrane alpha-helices, *Nat. Struct. Biol. 1*, 157−163.
43. Sulistijo, E. S., Jaszewski, T. M., and MacKenzie, K. R. (2003) Sequence-specific dimerization of the transmembrane domain of the "BH3-only" protein BNIP3 in membranes and detergent, *J. Biol. Chem. 278*, 51950−51956.
44. Doura, A. K., Kobus, F. J., Dubrovsky, L., Hibbard, E., and Fleming, K. G. (2004) Sequence context modulates the stability of a GxxxG-mediated transmembrane helix-helix dimer, *J. Mol. Biol. 341*, 991−998.
45. White, S. H., and Wimley, W. C. (1999) Membrane protein folding and stability: physical principles, *Annu. Rev. Biophys. Biomol. Struct. 28*, 319−365.
46. Burley, S. K., and Petsko, G. A. (1985) Aromatic-aromatic interaction: a mechanism of protein structure stabilization, *Science 229*, 23−28.
47. Deber, C. M., and Joshua, H. (1972) Side chain interactions in aromatic dipeptides, *Biopolymers 11*, 2493−2503.
48. Ruan, C., Yang, Z., Hallowita, N., and Rodgers, M. T. (2005) Cation-pi interactions with a model for the side chain of tryptophan: structures and absolute binding energies of alkali metal cation-indole complexes, *J. Phys. Chem. A 109*, 11539−11550.
49. Ruan, C., and Rodgers, M. T. (2004) Cation-pi interactions: structures and energetics of complexation of Na^+ and K^+ with the aromatic amino acids, phenylalanine, tyrosine, and tryptophan, *J. Am. Chem. Soc. 126*, 14600−14610.
50. Gallivan, J. P., and Dougherty, D. A. (1999) Cation-pi interactions in structural biology, *Proc. Natl. Acad. Sci. U.S.A. 96*, 9459−9464.
51. Schneider, D., and Engelman, D. M. (2003) GALLEX, a measurement of heterologous association of transmembrane helices in a biological membrane, *J. Biol. Chem. 278*, 3105−3111.
52. Adams, P. D., Engelman, D. M., and Brunger, A. T. (1996) Improved prediction for the structure of the dimeric transmembrane domain of glycophorin A obtained through global searching, *Proteins 26*, 257−261.
53. Adams, P. D., Arkin, I. T., Engelman, D. M., and Brunger, A. T. (1995) Computational searching and mutagenesis suggest a structure for the pentameric transmembrane domain of phospholamban, *Nat. Struct. Biol. 2*, 154−162.

BI7008773